JCTC Journal of Chemical Theory and Computation

Search for the $Li_n^{0/+1/-1}$ ($n = 5-7$) Lowest-Energy Structures Using the ab Initio Gradient Embedded Genetic Algorithm (GEGA). Elucidation of the Chemical Bonding in the Lithium Clusters

Anastassia N. Alexandrova and Alexander I. Boldyrev*

Department of Chemistry and Biochemistry, Utah State University, 0300 Old Main Hill, Logan, Utah 84322-0300

Received April 6, 2005

Abstract: We report the study of small lithium clusters $Li_n^{0/+1/-1}$ ($n = 5-7$), performed via the novel Gradient Embedded Genetic Algorithm (GEGA) technique and molecular orbital analysis. GEGA was developed for searching of the lowest-energy structures of clusters. Results of our search, obtained using this program, have been compared with the previous ab initio calculations, and the efficiency of the developed GEGA method has thus been confirmed. The molecular orbital analysis of the found $Li_n^{0/+1/-1}$ ($n = 5-7$) clusters showed the presence of multiple (σ and π) aromatic character in their chemical bonding, which governs their preferable shapes and special stability.

I. Introduction

The Genetic Algorithm (GA) is an optimization strategy based on the Darwinian evolution process.[1] Genetic Algorithms, simple methods which do not include the calculation of derivatives, were successfully used in many areas of science and technology when global optima for complex, many-parameter functions are needed to be found.[2,3] The search for global minima of chemical systems belongs to this class of problems and has been approached via GA techniques.[4−28] We developed a novel ab initio Gradient Embedded Genetic Algorithm program (GEGA), which combines the efficient features of the ab initio accuracy of obtained relative energies and geometries with a fast convergence rate. This was achieved by the application of the gradient-following technique and implementation of a specific mutation process. The algorithm was illustrated by its application to the search for global minima of small cationic, anionic and uncharged clusters of lithium Li_n ($n = 5-7$). The energies and geometries of the found lowest-energy structures were further refined using more accurate ab initio methods. Finally, analysis of the chemical bonding in the found global minimum species was performed.

The lithium clusters considered in this work have been previously studied experimentally[29,30] and, primarily, theoretically.[29−56] The first ionization potentials of the neutral cluster have been evaluated in photoelectron spectroscopic experiments.[29,30] Most of the authors agree on the structure of the global minima of such small clusters. Thus, the chosen clusters can serve as good testing systems for the developed GEGA program.

After the global minimum structures are found, the chemical bonding within them is analyzed, and the origin of their specific shapes is elucidated. Specifically, we introduce the concepts of aromaticity and antiaromaticity to the description of the chemical bonding in the considered alkali metal clusters. The concept of aromaticity was originally proposed for certain organic compounds possessing high symmetry and planar shape and containing $(4n+2)$ electrons in their π-molecular orbital system (Huckel's rule). Recently, the concept was advanced into organometallic[57−61] and all-metal systems.[62−71] Robinson's aromatic metal clusters[57−61] are only π-aromatic, while the all-metal clusters[62−71] are both π- and σ-aromatic. These examples have already shown the usefulness of the aromaticity concept in metal clusters, and we believe that the advances of the aromaticity concept further into metal and nonmetal clusters

* Corresponding author e-mail: boldyrev@cc.usu.edu.

10.1021/ct050093g CCC: $30.25
Published on Web 06/11/2005

will help us better understand chemical bonding, structure, and stability in these species as well as serve as a better interpretation of spectroscopic data. In our recent work, we presented our interpretation of the chemical bonding in small clusters of lithium and magnesium on the basis of the concept of pure σ-aromaticity.[72] In the current study, we extend the concepts of aromaticity and antiaromaticity of both σ- and π-types to larger lithium clusters, explaining their shape and stability.

II. Theoretical Methods

1. Genetic Algorithm Method. The GA-based search for the global minimum is performed in the 3*N* configurational space with the energy value as a criterion of the fit. Initially, for all individuals (structures) in the population (group of structures), the size of which is user-defined, the random generation of 3*N* Cartesian coordinates in the range [R_{min}; R_{max}] is performed. The R_{max} is calculated on the basis of the average interatomic distance in the cluster, defined by the user, and is adjusted to the dimensionality of the generated cluster. The minimum interatomic distance R_{min} is the smallest allowed interatomic distance, introduction of which prevents the program from generating unphysical solutions. The user can also specify the expected topology of the system ('compact', 'medium', or 'open') in order to adjust the [R_{min}; R_{max}] interval accordingly: the R_{max} evaluated by the program will be the smallest for 'compact' topologies, larger for 'medium', and the largest for 'open' topologies. This rough adjustment at the beginning of the execution allows faster convergence of the algorithm. However, it can only be done if there is some preliminary information available about preferable geometries of the studied type of systems. By default, the topology of the cluster is assumed to be 'open'. For homoatomic systems, such as lithium clusters, the initial generation of the population is performed in two steps. At first, a group of planar individuals, with one linear species included purposely, is randomly created. In the second step, three-dimensional individuals are generated. The two-step generation of the population is introduced, because the chance of planar and especially linear species to be randomly generated in the 3*N* space is very low compared to 3-D species. Our experience showed that such generation procedure guarantees a saturation of the population with planar, linear, and 3-D individuals and accelerates the overall convergence of the algorithm. Employing the Gaussian 03 package,[73] single-point energies are computed for all the species at the chosen level of theory (the user can define the method and the basis set). We used the (U)B3LYP[74−76] level with a small valence-split basis set 3-21G. Our experience showed that even using this level of theory, GEGA can predict the global minimum and the collection of the lowest-energy isomers quite accurately. Although the assignment of the global minimum structure may not always be accurate at this low level of theory in GEGA, we believe that the true global minimum will be among these low-energy isomers and may be identified later on by more sophisticated calculations following the GEGA search. The described meticulous initial selection of individuals is somewhat reminiscent of the Monte Carlo simulation.[77] The size of the population is recommended to be no less than 40 individuals for clusters containing up to seven atoms, in agreement with the previously suggested population size for this type of problem when the gradient-following technique is employed.[5] As we found, larger population size is computationally demanding while not necessary for the systems of such size. The population size should be increased for larger systems. At the moment we do not have detailed information about the performance of the GEGA depending on the population size. The criterion maintained in the code suggests the population size to be equal to or greater than 5*N*, where *N* is the number of atoms in the cluster. If the requested population size is smaller, then the warning message is printed out in the output file.

All the structures of the thus constructed initial population are then optimized to the nearest stationary points on the potential energy surface. If a saddle point is encountered, then the normal mode of the first imaginary frequency is followed until a local minimum is found. Further, the population, composed of the thus selected good individuals, undergoes breeding and mutations. The mating implemented in GEGA is performed on the basis of the robust technique originally proposed in 1995 by Deaven and Ho,[13] in which some of the geometrical features of good individuals in the population (parents) are combined and passed to new individuals (children). Parents are local minimum structures obtained either during the initial or subsequent iterations. Children are new structures made out of two parent structures. Probabilities to be bred (to produce child structures) are assigned to parents according to the best-fit (lowest-energy) criterion. Based on the probabilities, couples of parents are randomly selected. Figure 1A shows a typical breeding procedure on the example of selected structures of the Li_5^- cluster. The geometries of parents are cut by a random cutting plane (XY, YZ, or ZY), and the obtained halves (genes) are then recombined either in a simple or in a head-to-tail manner, forming a child. Figure 1A illustrates the case when the XY plane is chosen, and the recombination of the halves occurs in the simple manner, i.e., the part of geometry of the parent 1 taken from above the cutting plane is recombined with the part of geometry of the parent 2 taken from below the plane. The number of atoms in the newly generated geometry is checked, and the child is optimized to the nearest local minimum. If the number of atoms in the child is incorrect, the cutting plane is shifted so that the correct number of atoms results. After the number of individuals in the population is doubled within the breeding process, the best-fit group is selected and convergence of the algorithm is checked. The GEGA is considered converged if the current lowest-energy species (global minimum or, at least, a very stable local minimum) remains leading for 20 iterations. If the convergence is not yet met, the highest-energy species in the population undergo mutations. The mutation rate is set to 33.33%. Mutations are shifts of random atoms of a species in random directions, with the purpose of changing the initial geometry so as to push the structure out of the current local minimum to another well on the potential energy surface (see Figure 1B). Mutants are

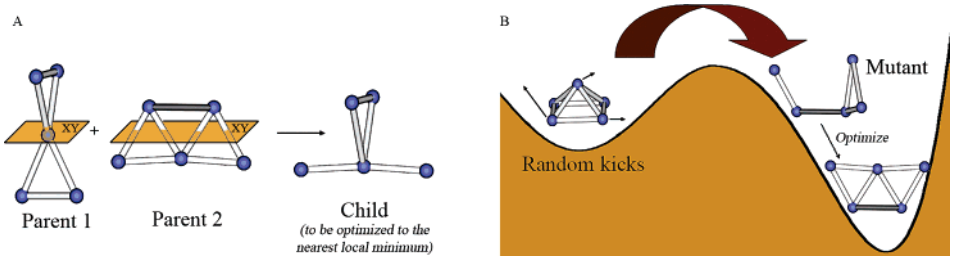

Figure 1. Illustration of the GEGA procedure: A. Breeding, when the XY plane is randomly chosen, geometries of two selected parents are cut by XY, and the parts of parents (the part of the parent 1 from above the plane and the part of the parent 2 from below the plane) are recombined in a simple manner; the obtained child will then be optimized to the nearest local minimum. B. Mutation, when the random number of kicks is introduced to distort the structure strongly enough to cross the barrier on the potential energy surface, the obtained mutant is then optimized to the local minimum.

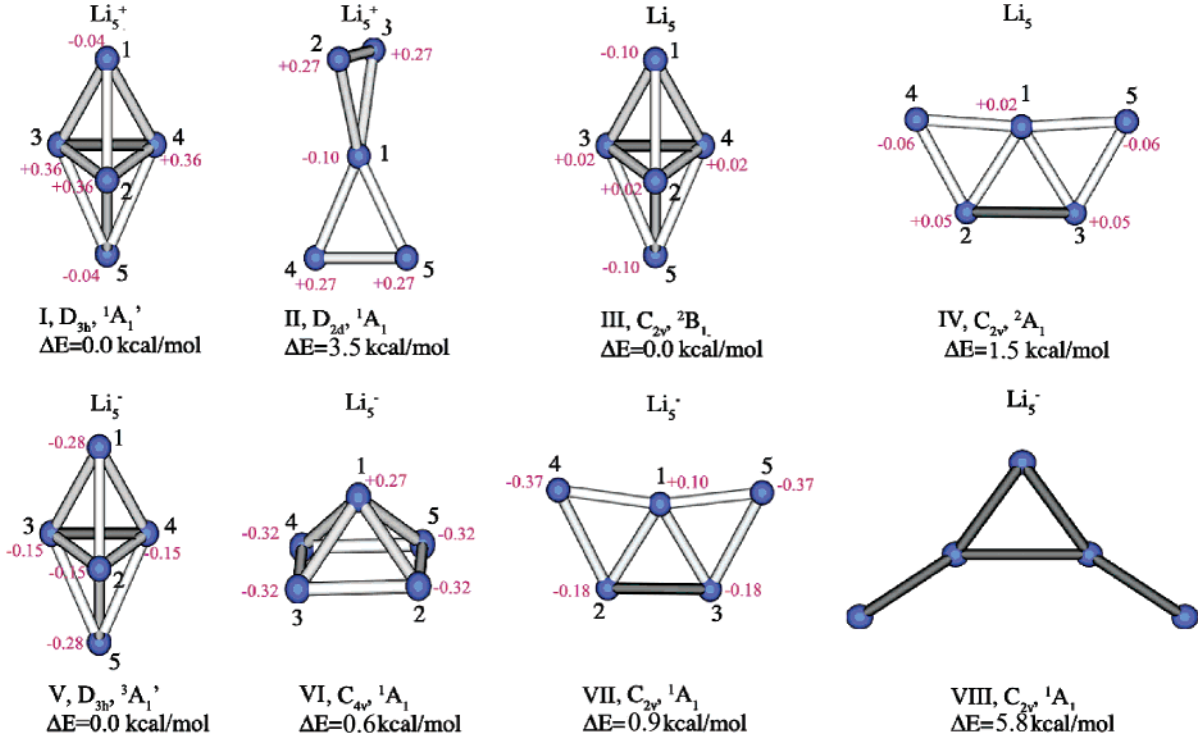

Figure 2. Global minimum and lowest in energy structures of Li_5^+, Li_5, and Li_5^- clusters found using the Genetic Algorithm. Shown geometries are refined at the CCSD(T)/6-311+G* level of theory. CCSD(T)/6-311+G(2df) ΔEs are given with ZPE corrections obtained at the CCSD(T)/6-311+G* level. The NPA atomic charges at the B3LYP/6-311+G* level are shown.

optimized to the nearest local minima. After mutations the algorithm proceeds with a new cycle of breeding. All low-lying isomers are detected and stored throughout the execution, and they are reported to the user at the end of the run. A few runs of GEGA are done on the system in order to confirm the found global minimum structure.

If high multiplicity states can be expected for a certain species, the GEGA search should be performed with different multiplicity values. For simpler systems it may be more reasonable to find the global minimum and isomers with the lowest possible multiplicity value and further manually check the lowest-energy structures with higher multiplicities.

According to our observations, the GEGA performance strongly depends on the calculated [R_{min}; R_{max}] interval. If the R_{max} is too small, imposing an unphysical restraint on the system, the global minimum will not be found. If the R_{max} is chosen to be too large, it is most likely that the convergence will eventually be met, but it will take much longer for the algorithm to converge. In the case of lithium clusters, as will be shown shortly, the geometries of the clusters are rather compact. Thus the specification of topology as 'compact' led to faster convergence to global minima. When 'medium' or 'open' topologies were chosen, the convergence was harder to reach. For example, in the case of the Li_7^+ cluster, 'compact' topology specification permitted the algorithm to converge within 22 iterations, while in the case of 'open' topology, 25 iterations were needed. Accurate average interatomic distance is always necessary for proper R_{max} assignment. On the other hand, if the R_{min} chosen by the user is very large, the performance of the GEGA can slow tremendously. This happens because many randomly generated geometries will have atom−atom distances falling within a large R_{min} and must therefore be discarded. As the number of atoms in the cluster increases, the likelihood of atom−atom distances falling within R_{min} increases, so GEGA can get stuck trying to generate physically eligible geometries. However, if the R_{min} is too

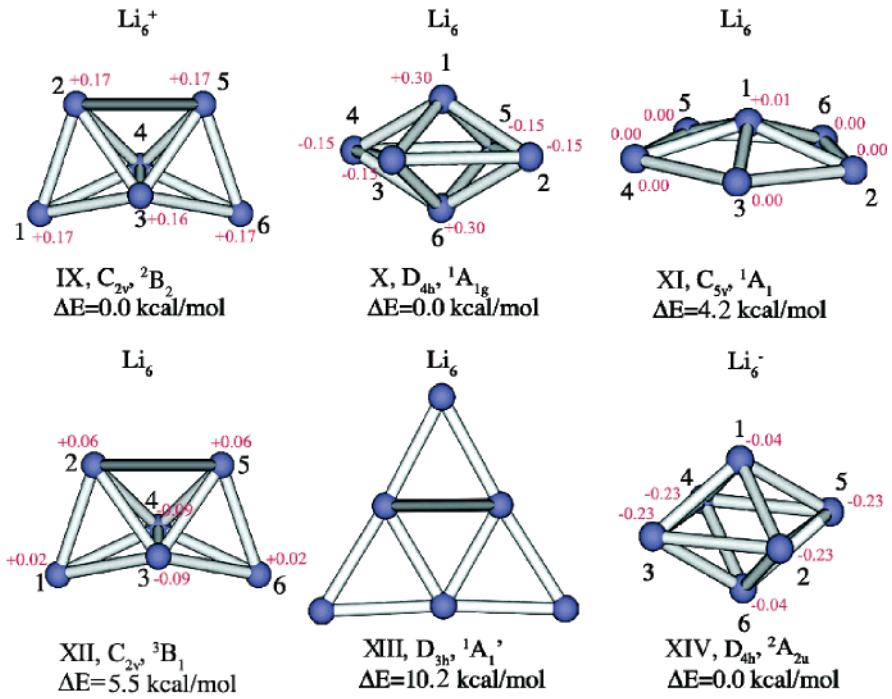

Figure 3. Global minimum and lowest in energy structures of Li_6^+, Li_6, and Li_6^- clusters found using the Genetic Algorithm. Shown geometries are refined at the CCSD(T)/6-311+G* level of theory. CCSD(T)/6-311+G(2df) ΔEs are given with ZPE corrections obtained at the CCSD(T)/6-311+G* level. The NPA atomic charges at the B3LYP/6-311+G* level are shown.

small, quantum chemical calculations may not reach SCF-convergence for some of the species.

So far, due to limited computational resources, we were not able to test our program on very large systems. However, the largest clusters to which GEGA was applied contained nine atoms (in the B3LYP/3-21G run) and 13 atoms (in the semiempirical run). With a new computer cluster (128 dual processors) we expect to extend the number of atoms in the GEGA search up to 20 or may be even 30 atoms.

2. Other Methods. After the global minima and lowest-energy isomers are found using the Genetic Algorithm program, geometries and energies of species are refined at the (U)B3LYP[74−76] and the coupled cluster (U)CCSD(T)[78−82] levels of theory with the more extended 6-311+G* basis set. The energies of the species are further refined at the (U)CCSD(T)/6-311+G(2df) + ZPE/CCSD(T)/6-311+G* level of theory. The first vertical and adiabatic ionization potentials were computed for all neutral and anionic global minima and compared to the available experimental data.[29,30] Chemical bonding analysis was performed using molecular orbital pictures (at the (U)HF/6-311+G* level) made with the MOLDEN program,[83] using natural population analysis (NPA)[84] at the (U)B3LYP/6-311+G* level and using the nucleus-independent chemical shifts (NICS)[85] calculated at the (U)B3LYP/6-311+G* level of theory. The diamagnetic and paramagnetic effects of the ring currents, associated with aromatic and antiaromatic compounds (i.e. shielding and deshielding of nuclei), respectively, can be measured by a simple criterion viz. NICS introduced by Schleyer and co-workers in 1996.[85] We employed NICS indices as a probe of aromaticity in our clusters in addition to the MO-analysis. All calculations were done using Gaussian 03 package.

III. Identified Lithium Clusters

We applied the designed GA for the search for the global minima of uncharged, cationic, and anionic small lithium clusters. The global minimum structures of the pentaatomic, hexaatomic, and heptaatomic clusters and their isomers found within 10 kcal/mol above the global minima, elucidated using the GEGA program, are shown in Figure 2−4, respectively. All calculated molecular properties are collected in Tables 1−9. The agreement between computational results obtained at the B3LYP and CCSD(T) methods is noteworthy.

Most of the previous theoretical works on the pentaatomic lithium clusters were devoted to the neutral Li_5 species (see for instance refs 33, 39, 41, and 47). All structures of Li_5 identified in this study have been found before, while their relative energies, depending on the applied computational method, varied.

The bipyramidal D_{3h} ($^1A_1'$) global minimum structure was found by the GEGA to be the global minimum of the Li_5^+ cluster (structure I, Figure 2). Its electronic configuration is $1a_1'^2 1a_2''^2$. The second isomer of the Li_5^+ cluster is the twisted D_{2d} ($^1A_1$) structure. It was found to be 3.5 kcal/mol above the global minimum at the CCSD(T)/6-311+G(2df) + ZPE/CCSD(T)/6-311+G* level of theory (structure II, Figure 2). The electronic configuration of this isomer is $1a_1^2 1b_2^2$.

The C_{2v} ($^2B_1$) isomer III was detected as a global minimum for the neutral Li_5 cluster at the B3LYP/3-21G level during the execution of the GEGA. From the GEGA calculations we found that the neutral Li_5 cluster has two low-lying isomers: the global minimum C_{2v} ($^2B_1$) (structure III, Figure 2) and isomer IV (C_{2v}, $^2A_1$). At the highest CCSD(T)/6-311+G(2df) + ZPE/CCSD(T)/6-311+G* level of theory the energy difference between these two isomers is 1.5 kcal/

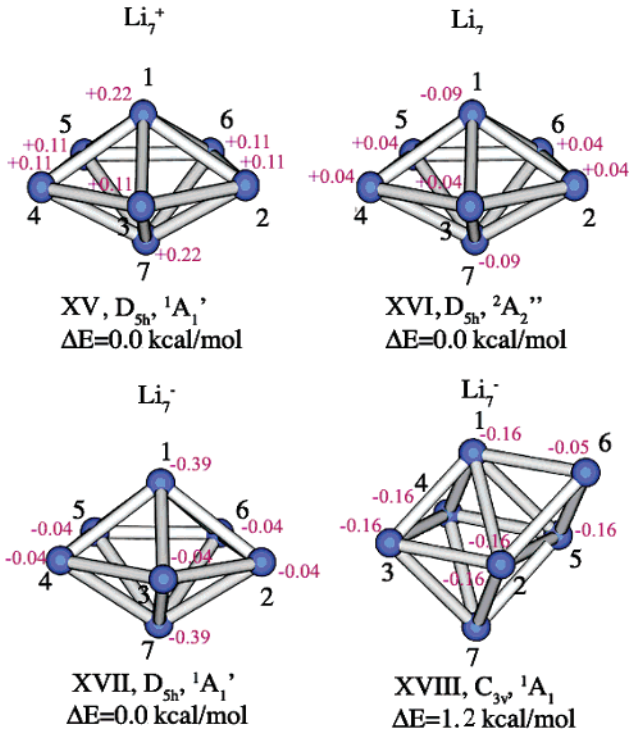

Figure 4. Global minimum and lowest in energy structures of Li_7^+, Li_7, and Li_7^- clusters found using the Genetic Algorithm. Shown geometries are refined at the CCSD(T)/6-311+G* level of theory. CCSD(T)/6-311+G(2df) ΔEs are given with ZPE corrections obtained at the CCSD(T)/6-311+G* level. The NPA atomic charges at the B3LYP/6-311+G* level are shown.

mol. The global minimum species has the $1a_1^2 1b_2^2 1b_1^1$ electronic configuration. The electronic configuration of the C_{2v} ($^2A_1$) species is the following: $1a_1^2 1b_2^2 2a_1^1$.

The GEGA run for the triplet state of the Li_5^- cluster revealed the bipyramidal D_{3h} species V to be the most stable. In the run of the GEGA for the singlet state we found the pyramidal C_{4v} species VI to have the lowest energy and the C_{2v} species VII to be the second isomer. At our highest level of theory (CCSD(T)/6-311+G(2df) + ZPE/CCSD(T)/6-311+G*) the global minimum of the Li_5^- cluster is the bipyramidal D_{3h} ($^3A_1'$) structure V (Figure 2), having the $1a_1'^2 1a_2''^2 1e'^2$ electronic configuration. The CCSD(T) calculation predicts structure VI (Figure 2) to be the second lowest-energy species (0.6 kcal/mol less stable than the global minimum) and structure VII to be 0.9 kcal/mol less stable. At this level of theory we cannot predict with certainty which of the structures V, VI, or VII is more stable. We conclude that the Li_5^- anion has three nearly degenerate most stable structures.

According to GEGA and calculations at higher levels of theory, the global minimum structure of the Li_6^+ cluster has C_{2v} ($^2B_2$) symmetry and the following electronic configuration: $1a_1^2 2a_1^2 1b_2^1$ (structure IX, Figure 3). This structure has also been found previously by Boustani et al.[47]

The neutral Li_6 cluster was found to have two low-energy isomers differing in energy by 4.2 kcal/mol at the CCSD(T)/6-311+G(2df) + ZPE/CCSD(T)/6-311+G* level of theory. The global minimum species (structure X, Figure 3)

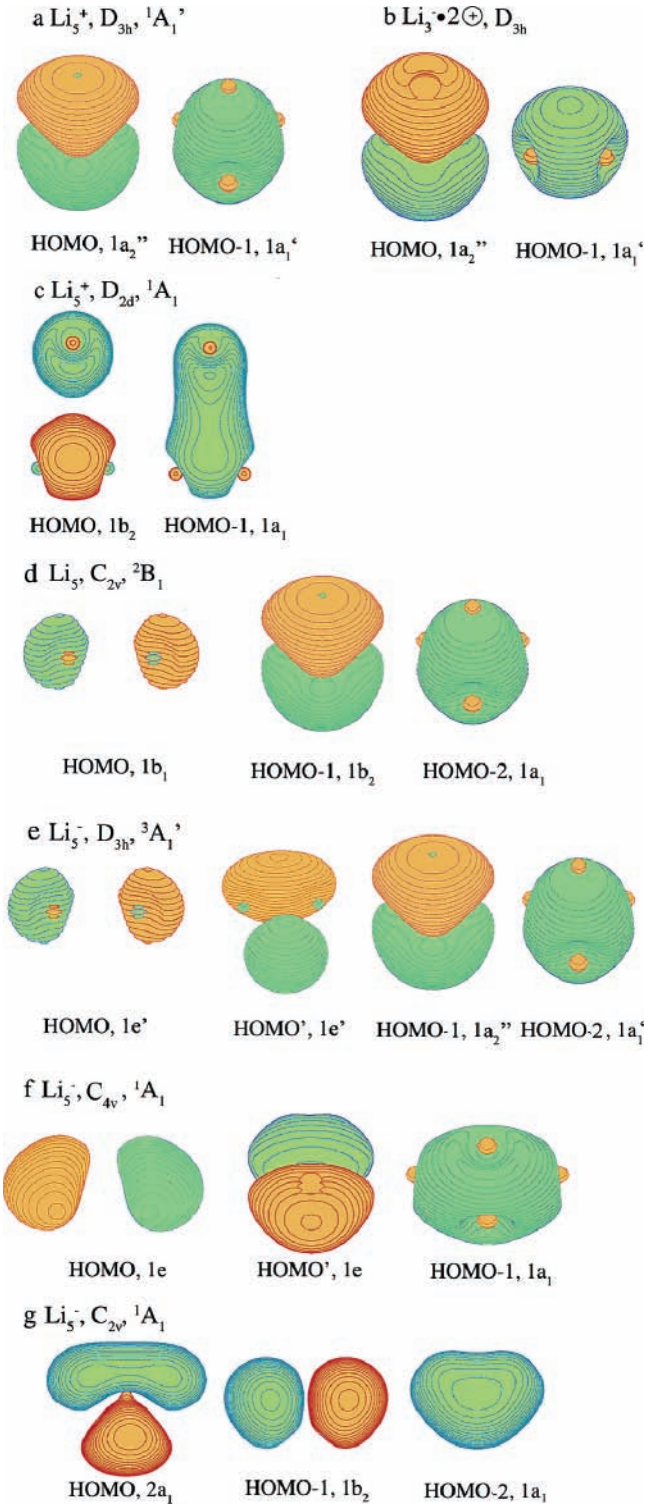

Figure 5. Molecular orbital picture of low-energy pentaatomic lithium clusters.

has D_{4h} ($^1A_{1g}$) symmetry and the $1a_{1g}^2 1e_u^4$ electronic configuration. The second isomer has C_{5v}, $^1A_1$ symmetry and corresponds to structure XI (Figure 3). The triplet species XII (C_{2v}, $^3B_1$) is the third most stable structure of the neutral Li_6 cluster (ΔE = 5.5 kcal/mol at the CCSD(T)/6-311+G(2df) + ZPE/CCSD(T)/6-311+G* level). The planar D_{3h} species XIII was found to be 10.2 kcal/mol (at CCSD(T)/6-311+G(2df) + ZPE/CCSD(T)/6-311+G*) above the global minimum. All detected structures were previously found

Table 1. Molecular Properties of the Li_5^+ Lowest-Energy Isomers

	Li_5^+, D_{3h}, $^1A_1'$		Li_5^+, D_{2d}, $^1A_1$	
level of theory	B3LYP/6-311+G*	CCSD(T)/6-311+G*	B3LYP/6-311+G*	CCSD(T)/6-311+G*
E_{total}, au	−37.428945	−37.145886[a]	−37.425738	−37.13911[b]
ZPE, kcal/mol	2.9	2.9	2.3	2.2
geometry	R(Li1−Li2) = 3.15 Å	R(Li1−Li2) = 3.16 Å	R(Li1−Li2) = 3.07 Å	R(Li1−Li2) = 3.11 Å
	R(Li2−Li3) = 2.69 Å	R(Li2−Li3) = 2.77 Å	R(Li2−Li3) = 2.82 Å	R(Li2−Li3) = 2.85 Å
frequencies	$\omega_1(a_1')$ 350 (0)[c]	$\omega_1(a_1')$ 329	$\omega_1(a_1)$ 318 (0)[c]	$\omega_1(a_1)$ 314
	$\omega_2(a_1')$ 237 (0)	$\omega_2(a_1')$ 236	$\omega_2(a_1)$139 (0)	$\omega_2(a_1)$135
	$\omega_3(a_2'')$ 300 (0)	$\omega_3(a_2'')$ 304	$\omega_3(b_1)$ 30 (0)	$\omega_3(b_1)$ 32
	$\omega_4(e')$ 278 (22)	$\omega_4(e')$ 257	$\omega_4(b_2)$ 329 (1)	$\omega_4(b_2)$ 326
	$\omega_5(e')$ 150 (2)	$\omega_5(e')$ 154	$\omega_5(b_2)$ 271 (60)	$\omega_5(b_2)$ 264
	$\omega_6(e'')$ 136 (0)	$\omega_6(e'')$ 156	$\omega_6(e)$ 219 (28)	$\omega_6(e)$ 208
			$\omega_7(e)$ 41 (4)	$\omega_7(e)$ 44

[a] At the CCSD(T)/6-311+G(2df) level the E_{total} = −37.151522 au. [b] At the CCSD(T)/6-311+G(2df) level the E_{total} = −37.1444574 au. [c] Infrared intensities in km/mol are shown in parentheses.

Table 2. Molecular Properties of the Li_5 Lowest-Energy Isomers

	Li_5, C_{2v}, $^2B_1$		Li_5, C_{2v}, $^2A_1$	
level of theory	B3LYP/6-311+G*	CCSD(T)/6-311+G*	B3LYP/6-311+G*	CCSD(T)/6-311+G*
E_{total}, au	−37.580450	−37.292976[a]	−37.578921	−37.291709[b]
ZPE, kcal/mol	2.7	2.6	2.5	2.5
geometry	R(Li1−Li2) = 2.97 Å	R(Li1−Li2) = 2.98 Å	R(Li2−Li4) = 2.97 Å	R(Li2−Li4) = 2.96 Å
	R(Li1−Li3,4) = 2.63 Å	R(Li1−Li3,4) = 2.72 Å	R(Li1−Li2,3) = 2.85 Å	R(Li1−Li2,3) = 2.94 Å
	R(Li2−Li3) = 3.05 Å	R(Li2−Li3) = 3.07 Å	R(Li1−Li4,5) = 2.98 Å	R(Li1−Li4,5) = 2.99 Å
	R(Li3−Li4) = 3.02 Å	R(Li3−Li4) = 3.07 Å	R(Li2−Li3) = 3.05 Å	R(Li2−Li3) = 3.11 Å
frequencies	$\omega_1(a_1)$ 348 (6)[c]	$\omega_1(a_1)$ 329	$\omega_1(a_1)$ 319 (20)[c]	$\omega_1(a_1)$ 292
	$\omega_2(a_1)$ 245 (1)	$\omega_2(a_1)$ 244	$\omega_2(a_1)$ 289 (0)	$\omega_2(a_1)$ 267
	$\omega_3(a_1)$ 209 (10)	$\omega_3(a_1)$ 205	$\omega_3(a_1)$ 184 (1)	$\omega_3(a_1)$ 185
	$\omega_4(a_2)$ 178 (0)	$\omega_4(a_2)$ 171	$\omega_4(a_1)$ 130 (3)	$\omega_4(a_1)$ 133
	$\omega_5(b_1)$ 160 (19)	$\omega_5(b_1)$ 167	$\omega_5(a_2)$ 69 (0)	$\omega_5(a_2)$ 69
	$\omega_6(b_1)$ 128 (1)	$\omega_6(b_1)$ 96	$\omega_6(b_1)$ 78 (8)	$\omega_6(b_1)$ 65
	$\omega_7(b_2)$ 284 (13)	$\omega_7(b_2)$ 288	$\omega_7(b_2)$ 277 (0)	$\omega_7(b_2)$ 342
	$\omega_8(b_2)$ 183 (1)	$\omega_8(b_2)$ 186	$\omega_8(b_2)$ 224 (5)	$\omega_8(b_2)$ 236
	$\omega_9(b_2)$ 162 (0)	$\omega_9(b_2)$ 161	$\omega_9(b_2)$ 184 (0)	$\omega_9(b_2)$ 182

[a] At the CCSD(T)/6-311+G(2df) level E_{total} =−37.298767 au. [b] At the CCSD(T)/6-311+G(2df) level E_{total} = −37.296434 au. [c] Infrared intensities in Km/mol are shown in parentheses.

by various research groups,[7,33,39,41,50] even though there were some contradictions on which one is the actual global minimum. However, the agreement between results obtained by the B3LYP/3-21G (GEGA run) and other higher levels of theory makes us more confident in our assignment of the relative energies of the Li_6 isomers. As we were about to send this paper to press, an article by Temelso and Sherrill came out.[56] The results of this work on the neutral, anionic, and cationic Li_6 clusters are in almost quantitative agreement with ours. Both cationic C_{2v} and anionic D_{4h} global minimum species found by the authors are the same as in our work. For the neutral Li_6 cluster the authors predicted the D_{4h} bipyramidal structure (analogous to our structure X, Figure 3) to be the most stable. The C_{5v} species was identified as the second isomer being 5.6 kcal/mol above the D_{4h} cluster at the most accurate CCSD(T)/cc-pCVQZ level, which is in good agreement with our number of 4.2 kcal/mol (CCSD(T)/6-311+G(2df) + ZPE/CCSD(T)/6-311+G* level). The planar D_{3h} species was found 7.6 kcal/mol higher in energy than the global minimum compared to our 10.2 kcal/mol (CCSD(T)/6-311+G(2df) + ZPE/CCSD(T)/6-311+G* level).

For the anionic Li_6^- cluster the global minimum structure is a tetragonal bipyramid D_{4h}, $^2A_{2u}$ (structure XIV, Figure 3). The bipyramid D_{4h}, $^2A_{2u}$ structure XIV can be traced to the bipyramid D_{4h}, $^1A_{1g}$ structure X upon addition of an electron to the LUMO of the neutral cluster. As the result of this addition, the tetragonal bipyramid is extended along the C4 axis, and it approaches an octahedral structure.

GEGA identified the global minimum structures of the Li_7^+, Li_7, and Li_7^- clusters all as pentagonal bipyramidals with D_{5h} symmetry (in Figure 4, structures XV, XVI, and XVII, respectively). This result was proved at the B3LYP/6-311G*, CCSD(T)/6-311+G*, and CCSD(T)/6-311+G(2df) + ZPE/CCSD(T)/6-311+G* levels. The electronic configurations of the cationic, neutral, and anionic species are $1a_1'^2 1e_1'^4$, $1a_1'^2 1e_1'^4 1a_2''^1$, and $1a_1'^2 1e_1'^4 1a_2''^2$, respectively. The anionic species also has a low-lying second isomer XVIII (C_{3v}, $^1A_1$) being just 1.2 kcal/mol above the global minimum. Its electronic configuration is $1a_1^2 2a_1^2 1e^4$. The found bipyramidal shape of the species agrees with previous reports.[39,41,47]

We have also calculated various properties of the found species. The predicted first ionization potentials for neutral species were found to be in a good agreement with the experimental photoelectron spectra.[29,30] For the distorted bipyramidal structure of the Li_5 cluster the calculated vertical

Table 3. Molecular Properties of the Li_5^- Lowest-Energy Isomers

	Li_5^-, D_{3h}, $^3A_1'$		Li_5^-, C_{4v}, $^1A_1$		Li_5^-, C_{2v}, $^1A_1$	
level of theory	B3LYP/6-311+G*	CCSD(T)/6-311+G*	B3LYP/6-311+G*	CCSD(T)/6-311+G*	B3LYP/6-311+G*	CCSD(T)/6-311+G*
E_{total}, au	−37.610893	−37.324953[a]	−37.608082	−37.323435[b]	−37.608840	−37.324138[c]
ZPE, kcal/mol	2.8	2.8	2.5	2.4	2.3	2.3
geometry	R(Li1−Li2,3,4) = 2.97 Å	R(Li1−Li2,3,4) = 3.01 Å	R(Li1−Li2) = 2.78 Å	R(Li1−Li2) = 2.84 Å	R(Li2−Li4) = 3.22 Å	R(Li2−Li4) = 3.24 Å
	R(Li2−Li3) = 2.85 Å	R(Li2−Li3) = 2.93 Å	R(Li2−Li3) = 3.21 Å	R(Li2−Li3) = 3.21 Å	R(Li1−Li2,3) = 2.89 Å	R(Li1−Li2,3) = 2.94 Å
					R(Li1−Li4,5) = 2.96 Å	R(Li1−Li4,5) = 2.99 Å
					R(Li2−Li3) = 2.95 Å	R(Li2−Li3) = 2.95 Å
frequencies	$\omega_1(a_1')$ 299 (0)[d]	$\omega_1(a_1')$ 287	$\omega_1(a_1)$ 298 (9)[d]	$\omega_1(a_1)$ 292	$\omega_1(a_1)$ 285 (24)[d]	$\omega_1(a_1)$ 285
	$\omega_2(a_1')$ 226 (0)	$\omega_2(a_1')$ 218	$\omega_2(a_1)$ 150 (4)	$\omega_2(a_1)$ 150	$\omega_2(a_1)$ 219 (4)	$\omega_2(a_1)$ 222
	$\omega_3(a_2'')$ 259 (18)	$\omega_3(a_2'')$ 262	$\omega_3(b_1)$ 180 (0)	$\omega_3(b_1)$ 182	$\omega_3(a_1)$ 182 (19)	$\omega_3(a_1)$ 180
	$\omega_4(e')$ 240 (0)	$\omega_4(e')$ 241	$\omega_4(b_2)$ 221 (0)	$\omega_4(b_2)$ 210	$\omega_4(a_1)$ 121 (0)	$\omega_4(a_1)$ 123
	$\omega_5(e')$ 201 (0)	$\omega_5(e')$ 231	$\omega_5(b_2)$ 73 (0)	$\omega_5(b_2)$ 55	$\omega_5(a_2)$ 93 (0)	$\omega_5(a_2)$ 88
	$\omega_6(e')$ 132 (1)	$\omega_6(e')$ 131	$\omega_6(e)$ 277 (27)	$\omega_6(e)$ 266	$\omega_6(b_1)$ 82 (1)	$\omega_6(b_1)$ 61
			$\omega_7(e)$ 134 (3)	$\omega_7(e)$ 128	$\omega_7(b_2)$ 298 (147)	$\omega_7(b_2)$ 298
					$\omega_8(b_2)$ 200 (3)	$\omega_8(b_2)$ 198
					$\omega_9(b_2)$ 149 (12)	$\omega_9(b_2)$ 144

[a] At the CCSD(T)/6-311+G(2df) level E_{total} = −37.331652 au. [b] At the CCSD(T)/6-311+G(2df) level E_{total} = −37.330154 au. [c] At the CCSD(T)/6-311+G(2df) level E_{total} = −37.329635 au. [d] Infrared intensities in km/mol are shown in parentheses.

ionization potential (IP) is 4.14 eV, and the theoretically predicted adiabatic IP is 4.00 eV. The experimental IP value was reported as 4.02 ± 0.1 eV.[29,30] The VDE_1 of the Li_5^- global minimum isomer V is 0.94 eV and the ADE = 0.87 eV. For the hexaatomic neutral D_{4h} bipyramid Li_6 the calculated vertical IP = 4.44 eV can be compared to the experimental IP = 4.20 ± 0.1 eV.[29,30] The VDE and ADE values for the Li_6^- D_{4h} ($^2A_{2u}$) structure XIV are 1.00 and 0.87 eV, respectively. For the pentagonal bipyramid Li_7 (D_{5h}, $^1A_1'$) the theoretical vertical IP = 4.08 eV and adiabatic IP = 3.95 eV can be compared to the experimental IP = 3.94 ± 0.1 eV.[29,30] Li_7^- (D_{5h}, $^1A_1'$) has VDE = 1.13 eV, and ADE = 0.80 eV.

Our calculated atomization energies per atom of the species are the following: Li_5^+ (D_{3h}, $^1A_1$) − 1.02 eV, Li_5 (C_{2v}, $^2B_1$) − 0.75 eV, Li_5 (C_{2v}, $^2A_1$) − 0.55 eV, Li_5^- (D_{3h}, $^3A_1'$) − 0.85 eV, Li_6^+ (C_{2v}, $^2A_1$) − 1.04 eV, Li_6 (D_{4h}, $^1A_{1g}$) − 0.86 eV, Li_6 (C_{5v}, $^1A_1$) − 0.83 eV, Li_6^- (D_{4h}, $^2A_{2u}$) − 0.92 eV, Li_7^+ (D_{5h}, $^1A_1'$) − 1.12 eV, Li_7 (D_{5h}, $^2A_2''$) − 0.92 eV, and Li_7^- (D_{5h}, $^1A_1'$) − 0.98 eV. These values can be compared to the atomization energy per atom of Li_2 − 0.52 eV.[86] They clearly show the enhanced stability in all clusters.

IV. Chemical Bonding in Lithium Clusters

To elucidate the nature of the chemical bonding in lithium clusters we used the molecular orbital analysis and NICS indices.

$Li_5^{+1/0/-1}$. Figure 5 contains MO pictures of the low-energy pentaatomic lithium clusters. The set of valence molecular orbitals of the bipyramidal D_{3h} global minimum structure of Li_5^+ is shown in Figure 5a. The HOMO-1 ($1a_1$) is a completely bonding σ-molecular orbital composed mostly of 2s-atomic orbitals on all five Li atoms. The HOMO ($1a_2$) is a completely bonding molecular orbital of π-character. It is composed of 2p atomic orbitals of three Li atoms in the base of the pyramid and 2s atomic orbitals of the two apex Li atoms. To prove the π-character of the HOMO, we calculated the cluster composed of three Li atoms in the base of the pyramid and two positive charges substituting the apex Li atoms. The molecular orbitals of this model system are shown in Figure 5b. As one can see the overall look of the molecular orbitals of the Li_3^- triangular base of the pyramid with two positive point-charges above and below the plane is the same as the look of the orbitals of the Li_5^+ pyramidal cluster. Both the π-character of the HOMO and the σ-character of the HOMO-1 are preserved when the contribution from 2s-functions on the apex Li atoms are completely excluded. This fact shows that the chemical bonding in the global Li_5^+ minimum can be described in terms of 2σ and 2π electrons present. Thus, according to the ($4n$+2) Hückel's rule, the species is both σ- and π-aromatic.[87] The doubly aromatic character[87] of the chemical bonding is responsible for the extra stability of the Li_5^+ global minimum isomer. What is unusual about chemical bonding in this cluster is an early occupation of the π-MO, i.e., the π-MO is occupied before the full set of σ-orbitals, required for the classical 2c-2e bonding among equatorial Li atoms, has been populated. However, such early occupation of π-MO in metal systems was already observed in the Al_4^{2-} cluster.[92]

Molecular orbitals of the second isomer of the Li_5^+ cluster are shown in Figure 5c. Both molecular orbitals of the twisted D_{2d} structure have σ-character. In fact the structure is a result of the fusion of two Li_3^+ triangular motifs sharing one atom. The Li_3^+ cluster has been reported to have only one completely bonding σ-molecular orbital and to be σ-aromatic.[72] The HOMO and HOMO-1 are linear combinations of the two completely bonding σ-molecular orbitals of the Li_3^+ units. Thus, the system can be defined as island aromatic, in the sense that the fusion of the two aromatic fragments is observed, and both individual aromatic units preserve their aromaticity inside the Li_5^+ D_{2d} structure.

Molecular orbitals of the (C_{2v}, $^2B_1$) global minimum isomer of the neutral Li_5 cluster are shown in Figure 5d. Two molecular orbitals (HOMO-1 ($1b_2$) and HOMO-2 ($1a_1$)) are reminiscent to HOMO ($1b_2$) and HOMO-1 ($1a_1$), respectively, of the Li_5^+ D_{3h} pyramidal species. However, the

Table 4. Molecular Properties of the Li_6^+, C_{2v}, $^2B_2$ Global Minimum Structure

level of theory	B3LYP/6-311+G*		CCSD(T)/6-311+G*	
E_{total}, au	−44.960548		−44.618696[a]	
ZPE, kcal/mol	3.6		3.6	
geometry	R(Li1−Li2) = 3.08 Å	R(Li2−Li5) = 3.36 Å	R(Li1−Li2) = 3.10 Å	R(Li2−Li5) = 3.44 Å
	R(Li1−Li3,4) = 3.06 Å	R(Li3−Li4) = 2.53 Å	R(Li1−Li3,4) = 3.00 Å	R(Li3−Li4) = 2.61 Å
	R(Li2−Li3,4) = 2.93 Å		R(Li2−Li3,4) = 3.10 Å	
frequencies	$\omega_1(a_1)$ 349 (4)[b]	$\omega_7(a_2)$ 144 (0)	$\omega_1(a_1)$ 330	$\omega_7(a_2)$ 142
	$\omega_2(a_1)$ 266 (22)	$\omega_8(b_1)$ 176 (6)	$\omega_2(a_1)$ 261	$\omega_8(b_1)$ 175
	$\omega_3(a_1)$ 253 (18)	$\omega_9(b_1)$ 153 (0)	$\omega_3(a_1)$ 251	$\omega_9(b_1)$ 155
	$\omega_4(a_1)$ 190 (0)	$\omega_{10}(b_2)$ 304 (19)	$\omega_4(a_1)$ 187	$\omega_{10}(b_2)$ 305
	$\omega_5(a_1)$ 88 (0)	$\omega_{11}(b_2)$ 212 (1)	$\omega_5(a_1)$ 81	$\omega_{11}(b_2)$ 215
	$\omega_6(a_2)$ 212 (0)	$\omega_{12}(b_2)$ 194 (4)	$\omega_6(a_2)$ 219	$\omega_{12}(b_2)$ 198

[a] At the CCSD(T)/6-311+G(2df) level E_{total} = −44.624912 au. [b] Infrared intensities in km/mol are shown in parentheses.

Table 5. Molecular Properties of the Li_6 Lowest-Energy Isomers

	Li_6, D_{4h}, $^1A_{1g}$		Li_6, C_{5v}, $^1A_1$		Li_6, C_{2v}, $^3B_1$	
level of theory	B3LYP/6-311+G*	CCSD(T)/6-311+G*	B3LYP/6-311+G*	CCSD(T)/6-311+G*	B3LYP/6-311+G*	CCSD(T)/6-311+G*
E_{total}, au	−45.116806	−44.774798[a]	−45.111046	−44.768332[b]	−45.110032	−44.767231[c]
ZPE, kcal/mol	3.8	3.7	3.3	3.2	3.8	3.7
geometry	R(Li1−Li2) = 3.05 Å	R(Li1−Li2) = 3.08 Å	R(Li1−Li2) = 2.79 Å	R(Li1−Li2) = 2.87 Å	R(Li1−Li2) = 2.91 Å	R(Li1−Li2) = 2.95 Å
	R(Li2−Li3) = 2.80 Å	R(Li2−Li3) = 2.81 Å	R(Li2−Li3) = 3.14 Å	R(Li2−Li3) = 3.14 Å	R(Li1−Li3,4) = 2.97 Å	R(Li1−Li3,4) = 3.02 Å
					R(Li2−Li3,4) = 2.86 Å	R(Li2−Li3,4) = 2.92 Å
					R(Li2−Li5) = 3.03 Å	R(Li2−Li5) = 3.11 Å
					R(Li3−Li4) = 2.85 Å	R(Li3−Li4) = 2.94 Å
frequencies	$\omega_1(a_{1g})$ 352 (0)[d]	$\omega_1(a_{1g})$ 326	$\omega_1(a_1)$ 254 (2)[d]	$\omega_1(a_1)$ 257	$\omega_1(a_1)$ 310 (4)[d]	$\omega_1(a_1)$ 302
	$\omega_2(a_{1g})$ 227 (0)	$\omega_2(a_{1g})$ 206	$\omega_2(a_1)$ 85 (4)	$\omega_2(a_1)$ 109	$\omega_2(a_1)$ 277 (14)	$\omega_2(a_1)$ 274
	$\omega_3(a_{2u})$ 205 (5)	$\omega_3(a_{2u})$ 206	$\omega_3(e_1)$ 345 (1)	$\omega_3(e_1)$ 323	$\omega_3(a_1)$ 245 (10)	$\omega_3(a_1)$ 236
	$\omega_4(b_{1g})$ 270 (0)	$\omega_4(b_{1g})$ 263	$\omega_4(e_1)$ 178 (2)	$\omega_4(e_1)$ 182	$\omega_4(a_1)$ 205 (1)	$\omega_4(a_1)$ 197
	$\omega_5(b_{2g})$ 121 (0)	$\omega_5(b_{2g})$ 114	$\omega_5(e_2)$ 203 (0)	$\omega_5(e_2)$ 197	$\omega_5(a_1)$ 97 (0)	$\omega_5(a_1)$ 95
	$\omega_6(b_{2u})$ 179 (0)	$\omega_6(b_{2u})$ 179	$\omega_6(e_2)$ 192 (0)	$\omega_6(e_2)$ 192	$\omega_6(a_2)$ 246 (0)	$\omega_6(a_2)$ 240
	$\omega_7(e_g)$ 254 (0)	$\omega_7(e_g)$ 251	$\omega_7(e_2)$ 58 (0)	$\omega_7(e_2)$ 45	$\omega_&(a_2)$ 125 (0)	$\omega_&(a_2)$ 125
	$\omega_8(e_u)$ 331 (3)	$\omega_8(e_u)$ 328			$\omega_8(b_1)$ 250 (13)	$\omega_8(b_1)$ 244
	$\omega_9(e_u)$ 60 (0)	$\omega_9(e_u)$ 51			$\omega_9(b_1)$ 155 (15)	$\omega_9(b_1)$ 167
					$\omega_{10}(b_2)$ 302 (28)	$\omega_{10}(b_2)$ 309
					$\omega_{11}(b_2)$ 219 (2)	$\omega_{11}(b_2)$ 223
					$\omega_{12}(b_2)$ 197 (0)	$\omega_{12}(b_2)$ 202

[a] At the CCSD(T)/6-311+G(2df) level E_{total} = −44.782932 au. [b] At the CCSD(T)/6-311+G(2df) level E_{total} = −44.774803 au. [c] At the CCSD(T)/6-311+G(2df) level E_{total} = −44.774103 au. [d] Infrared intensities in km/mol are shown in parentheses.

HOMO ($1b_1$) in the C_{2v} global minimum structure of Li_5 is a nonbonding σ-molecular orbital. It belongs to the quasi-degenerate pair of σ-molecular orbitals, with counterpart as the LUMO. A Jahn−Teller distortion, thus imposed, results in the lower C_{2v} symmetry of the cluster. The system contains two π-electrons analogous to the Li_5^+ D_{3h} species, obeys the $(4n+2)$ rule, and, consequently, is π-aromatic. The described partial occupation of the σ-set (the completely bonding HOMO-2 and the nonbonding HOMO) makes the system σ-antiaromatic. Adding an electron leads to the double population of the degenerate HOMO and a gain of σ-aromaticity.

The pattern of the molecular orbitals in the second C_{2v} ($^2A_1$) isomer of Li_5 is very similar to the C_{2v} isomer VII of the Li_5^- cluster, which has an electronic configuration $1a_1^2 1b_2^2 2a_1^2$. The neutral and anionic clusters only differ in the number of electrons occupying the HOMO. Let us first consider the chemical bonding in the closed-shell anionic species.

The planar C_{2v}, $^1A_1$ species is the third lowest-energy isomer of the Li_5^- cluster (structure VII, Figure 2). The molecular orbitals of this cluster are shown in Figure 5g. All three occupied molecular orbitals have σ-character. The HOMO-2 is a completely bonding σ-molecular orbital, while the HOMO and the HOMO-1 are partially bonding σ-MOs. The set of bonding σ-molecular orbitals in this isomer of Li_5^- is completely filled by 6 σ-electrons, which, at first glance, should lead to perfect D_{5h} symmetry and σ-aromaticity due to the $(4n+2)$ rule. However, the perfectly symmetric D_{5h} structure is a second-order saddle point on the potential energy surface, and the imaginary frequency normal mode leads to the found C_{2v} species. This contradiction has been resolved via the analysis of the composition of the molecular orbitals in the species. It showed that all molecular orbitals, although mostly composed of 2s-atomic orbitals of Li atoms, have a significant contribution from 2p-atomic orbitals, and thus should be considered as hybridized. The hybridization enhances the overlap and the overall bonding character of the HOMO and HOMO-1. In the HOMO a large contribution to the bonding comes from the overlap of the σ-cloud on atoms Li2 and Li3 with the p_z-atomic orbital of the Li1 atom perpendicular to this cloud, which can be observed from the molecular orbital picture. If no 2p-contribution would occur, there would be no bonding

Table 6. Molecular Properties of the Li_6^-, D_{4h}, $^2A_{2u}$ Global Minimum Structure

level of theory	B3LYP/6-311+G*	CCSD(T)/6-311+G*
E_{total}, au	−45.147179	−44.806674[a]
ZPE, kcal/mol	3.6	3.6
geometry	R(Li1−Li2) = 2.81 Å	R(Li1−Li2) = 2.88 Å
	R(Li2−Li3) = 3.34 Å	R(Li2−Li3) = 3.35 Å
frequencies	$\omega_1(a_{1g})$ 301 (6)[b]	$\omega_1(a_{1g})$ 301
	$\omega_2(a_{1g})$ 156 (3)	$\omega_2(a_{1g})$ 141
	$\omega_3(a_{2u})$ 191 (2)	$\omega_3(a_{2u})$ 236
	$\omega_4(b_{1g})$ 248 (0)	$\omega_4(b_{1g})$ 286
	$\omega_5(b_{2g})$ 143 (0)	$\omega_5(b_{2g})$ 130
	$\omega_6(b_{2u})$ 166 (0)	$\omega_6(b_{2u})$ 233
	$\omega_7(e_g)$ 254 (0)	$\omega_7(e_g)$ 238
	$\omega_8(e_u)$ 298 (3)	$\omega_8(e_u)$ 292
	$\omega_9(e_u)$ 89 (1)	$\omega_9(e_u)$ 84

[a] At the CCSD(T)/6-311+G(2df) level E_{total} = −44.815330 au. [b] Infrared intensities in km/mol are shown in parentheses.

character between the Li1 atom and the σ-cloud on atoms Li2 and Li3, because in the original σ-molecular orbital they are divided by a nodal plane. Thus, the hybridization brings an additional bonding to the system across the nodal plane of the HOMO and causes a structural distortion from D_{5h} symmetry to C_{2v} by drawing Li1 toward Li2 and Li3. Quantitatively, this phenomenon can be described by the expansion of the HOMO in terms of AOs on atoms. At the RHF/6-311+G* level the portion of the expansion coming from the Li1 atom is the following: $0.002(1s) + 0.028(2s) - 0.046(2p_z) - 0.069(3s) - 0.093(3p_z) - 0.015(4s) - 0.039(4p_z) - 0.199(5s) + 0.109(5p_z) + 0.012(6d_0) + 0.008(6d_{2+})$, which shows that the majority of electron density on Li1 comes from the p_z-originated atomic orbitals. In the HOMO-1, Li1 carries a p_y-contribution across the nodal plane. Li1 brings the following portion to the expansion of the HOMO-1 (RHF/6-311+G* level): $0.07(2p_y) + 0.150(3p_y) - 0.187(4p_y) + 0.081(5p_y) - 0.004(6d_{-1})$. It is important, that if no p-character would exist in HOMO-1, the coefficients in the HOMO-1 expansion, corresponding to the functions on the Li1 atom, would be zero. To check the validity of such an explanation of the chemical bonding in Li_5^- (C_{2v}, $^1A_1$), we artificially removed the p-functions from the atoms and calculated the D_{5h} perfectly symmetric structure. In this case, when there are no p-contributions to molecular orbitals, the Li_5^- D_{5h} species is a true minimum on the potential energy surface.

The chemical bonding in the previously mentioned second C_{2v} isomer of the Li_5 neutral cluster (structure IV, Figure 2), having a similar structure to the third isomer of Li_5^-, can be described in the same manner. The s−p hybridization leads to the strong distortion of the cluster toward C_{2v} symmetry. However, this structural rearrangement is smaller than in the third isomer of Li_5^- (see Tables 2 and 3 to compare geometries), because the HOMO in Li_5 is populated with one electron only, and thus the bonding brought to the system by the HOMO is less.

At the highest applied level of theory (CCSD(T)/6-311+G(2df)) the global minimum of the Li_5^- cluster is a bipyramidal structure V (Figure 2). The $1a_1'^2 1a_2''^2 1e'^2$ electronic configuration of the species corresponds to the population of the σ-bonding set of molecular orbitals (Figure 5e) in the base

Table 7. Molecular Properties of the Li_7^+, D_{5h}, $^1A_1'$ Global Minimum Structure

level of theory	B3LYP/6-311+G*	CCSD(T)/6-311+G*
E_{total}, au	−52.506609	−52.108467[a]
ZPE, kcal/mol	4.7	4.5
geometry	R(Li1−Li2) = 2.78 Å	R(Li1−Li2) = 2.74 Å
	R(Li2−Li3) = 3.06 Å	R(Li2−Li3) = 3.02 Å
frequencies	$\omega_1(a_1')$ 364 (0)[b]	$\omega_1(a_1')$ 338
	$\omega_2(a_1')$ 245 (0)	$\omega_2(a_1')$ 239
	$\omega_3(a_2'')$ 174 (1)	$\omega_3(a_2'')$ 168
	$\omega_4(e_1')$ 304 (37)	$\omega_4(e_1')$ 298
	$\omega_5(e_1')$ 171 (2)	$\omega_5(e_1')$ 168
	$\omega_6(e_2')$ 213 (0)	$\omega_6(e_2')$ 224
	$\omega_7(e_2')$ 198 (0)	$\omega_7(e_2')$ 207
	$\omega_8(e_2'')$ 227 (0)	$\omega_8(e_2'')$ 187
	$\omega_9(e_2'')$ 133 (0)	$\omega_9(e_2'')$ 129

[a] At the CCSD(T)/6-311+G(2df) level E_{total} = −52.116856 au. [b] Infrared intensities in Km/mol are shown in parentheses.

Table 8. Molecular Properties of the Li_7, D_{5h}, $^2A_2''$ Global Minimum Structure

level of theory	B3LYP/6-311+G*	CCSD(T)/6-311+G*
E_{total}, au	−52.652085	−52.253634[a]
ZPE, kcal/mol	4.7	5.7
geometry	R(Li1−Li2,3,4,5) = 2.91 Å	R(Li1−Li2,3,4,5) = 2.97 Å
	R(Li2−Li3) = 3.02 Å	R(Li2−Li3) = 3.06 Å
frequencies	$\omega_1(a_1')$ 301 (0)[b]	$\omega_1(a_1')$ 288
	$\omega_2(a_1')$ 235 (0)	$\omega_2(a_1')$ 218
	$\omega_3(a_2'')$ 165 (28)	$\omega_3(a_2'')$ 217
	$\omega_4(e_1')$ 304 (29)	$\omega_4(e_1')$ 495
	$\omega_5(e_1')$ 184 (4)	$\omega_5(e_1')$ 202
	$\omega_6(e_2')$ 237 (0)	$\omega_6(e_2')$ 231
	$\omega_7(e_2')$ 208 (0)	$\omega_7(e_2')$ 230
	$\omega_8(e_2'')$ 254 (0)	$\omega_8(e_2'')$ 301
	$\omega_9(e_2'')$ 104 (0)	$\omega_9(e_2'')$ 181

[a] At the CCSD(T)/6-311+G(2df) level E_{total} = −52.262340 au. [b] Infrared intensities in km/mol are shown in parentheses.

of the bipyramid. The completely bonding HOMO-2 and the doubly degenerate nonbonding HOMO contain four σ-electrons. The bipyramidal global minimum is σ-aromatic according to the $4n$ rule for triplets.[93] However, this structure is also a π-aromatic system due to the doubly occupied HOMO-1, and thus overall it is a doubly aromatic system. The pyramidal C_{4v} isomer VI (Figure 2) contains six electrons in three σ-molecular orbitals (Figure 5f). Thus this closed-shell cluster is σ-aromatic according to the regular $4n+2$ Hückel's rule.

We also used NICS indices as additional criteria of aromatic or antiaromatic character of the identified global minima. The computed indices are shown in Table 10. However, as one may see, in the case of pentaatomic lithium clusters, our conclusion about the double aromaticity of Li_5^+ (D_{3h}, $^1A_1'$ species I, Figure 2), the σ-antiaromaticity and π-aromaticity of Li_5 (C_{2v}, $^2B_1$ species III, Figure 2), and the double aromaticity of the triplet Li_5^- (cluster V, Figure 2) completely disagrees with the obtained NICS values (negative NICS indices correspond to aromatic character, positive to antiaromatic).

$Li_6^{+1/0/-1}$. MOs of hexaatomic clusters are given in Figure 6. Let us first consider chemical bonding in the neutral Li_6 cluster.

The global minimum of the neutral Li_6 (D_{4h}, $^1A_{1g}$) cluster X has a completely bonding σ-molecular orbital HOMO-1

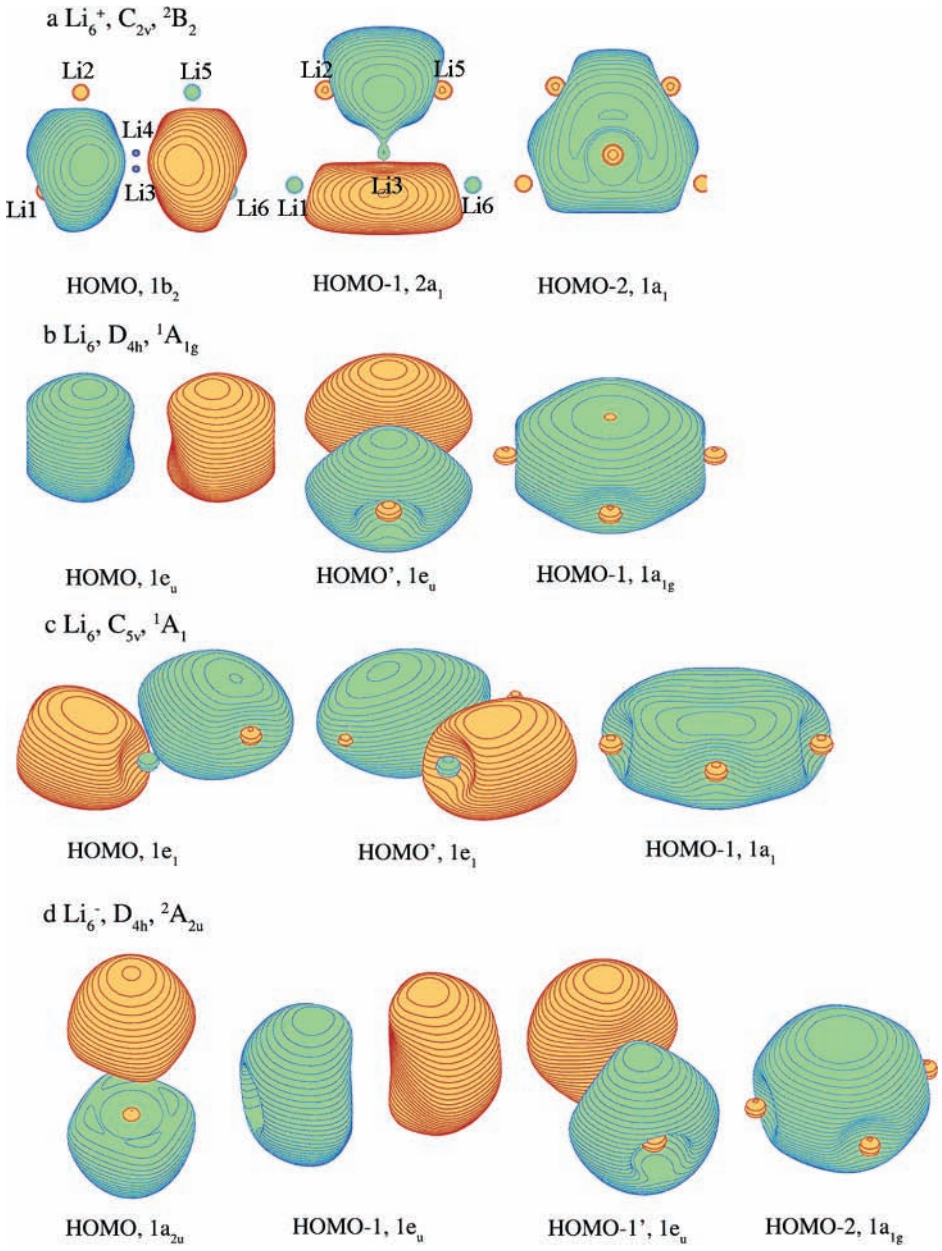

Figure 6. Molecular orbital picture of low-energy hexaatomic lithium clusters.

($1a_{1g}$) (see Figure 6b). The doubly degenerate HOMO has σ-character too with a major contributions from the 2s-functions of the equatorial Li atoms. The system thus contains six σ-electrons and is σ-aromatic.

Figure 6c depicts the molecular orbitals of the second quasi-planar isomer XI (Figure 3) (C_{5v}, $^1A_1$) of the Li_6 cluster. As one may see all electron density in the species is concentrated on the base of the pyramid, while no electron density is observed at the apex Li atom. All molecular orbitals have σ-character and align in the plane of the base of the pyramid. The completely bonding HOMO-1 ($1a_1$) and the partially bonding doubly degenerate HOMO ($1e_1$) form the σ-bonding set. Having six σ-electrons occupying these molecular orbitals the system is σ-aromatic.

Now we can easily interpret molecular orbitals of the global minimum Li_6^+ species (C_{2v}, $^2A_1$ structure IX, Figure 3), which are shown in Figure 6a. We can relate the MOs in Li_6^+ IX to the MOs in Li_6 X. HOMO in Li_6^+ is originated from HOMO in Li_6, HOMO-1 in Li_6^+ is originated from HOMO′ in Li_6, and HOMO-2 in Li_6^+ is originated from HOMO-1 in Li_6. The occupation by three electrons of the doubly degenerate HOMO in the D_{4h} structure leads to a Jahn−Teller distortion toward the C_{2v}, $^2A_1$ structure IX, Figure 3.

The global minimum of Li_6^- has molecular orbitals (shown in Figure 6d) very similar to its neutral structural analogue X (Figure 3). In this case the LUMO in Li_6 (which is the last member of the triply degenerate set of molecular orbitals) is occupied with one electron. The system approaches the perfect octahedral symmetry with atoms Li1 and Li6 being found farther apart than in the neutral species X. The system still possesses σ-aromatic character of the chemical bonding due to the occupation of the HOMO-2 ($1a_{1g}$) and HOMO-1

Table 9. Molecular Properties of the Li_7^- Global Minimum and the Second Lowest-Energy Isomer

	Li_7^-, D_{5h}, $^1A_1'$		Li_7^-, C_{3v}, $^1A_1$	
level of theory	B3LYP/6-311+G*	CCSD(T)/6-311+G*	B3LYP/6-311+G*	CCSD(T)/6-311+G*
E_{total}, au	−52.680731	−52.289214[a]	−52.679888	−52.282973[b]
ZPE, kcal/mol	4.4	4.3	4.3	4.3
geometry	R(Li1−Li2,3,4,5) = 2.98 Å	R(Li1−Li2,3,4,5) = 3.04 Å	R(Li6−Li1,2,5) = 2.94 Å	R(Li6−Li1,2,5) = 2.97 Å
	R(Li2−Li3) = 2.89 Å	R(Li2−Li3) = 2.92 Å	R(Li1−Li2) = 3.03 Å	R(Li1−Li2) = 3.11 Å
			R(Li1−Li3) = 2.88 Å	R(Li1−Li3) = 2.93 Å
			R(Li3−Li4) = 3.08 Å	R(Li3−Li4) = 3.12 Å
frequencies	$\omega_1(a_1')$ 275 (0)[c]	$\omega_1(a_1')$ 269	$\omega_1(a_1)$ 306 (2)[c]	$\omega_1(a_1)$ 302
	$\omega_2(a_1')$ 140 (0)	$\omega_2(a_1')$ 145	$\omega_2(a_1)$ 263 (0)	$\omega_2(a_1)$ 260
	$\omega_3(a_2'')$ 189(12)	$\omega_3(a_2'')$ 197	$\omega_3(a_1)$ 211 (1)	$\omega_3(a_1)$ 212
	$\omega_4(e_1')$ 279 (1)	$\omega_4(e_1')$ 276	$\omega_4(a_1)$ 182 (5)	$\omega_4(a_1)$ 174
	$\omega_5(e_1')$ 191 (1)	$\omega_5(e_1')$ 186	$\omega_5(a_2)$ 188 (0)	$\omega_5(a_2)$ 185
	$\omega_6(e_2')$ 170 (0)	$\omega_6(e_2')$ 166	$\omega_6(e)$ 276 (0)	$\omega_6(e)$ 277
	$\omega_7(e_2')$ 250 (0)	$\omega_7(e_2')$ 269	$\omega_7(e)$ 251 (3)	$\omega_7(e)$ 249
	$\omega_8(e_2'')$ 267 (0)	$\omega_8(e_2'')$ 239	$\omega_8(e)$ 180 (1)	$\omega_8(e)$ 183
	$\omega_9(e_2'')$ 91.(0)	$\omega_9(e_2'')$ 77	$\omega_9(e)$ 131 (2)	$\omega_9(e)$ 129
			$\omega_{10}(e)$ 101 (3)	$\omega_{10}(e)$ 101

[a] At the CCSD(T)/6-311+G(2df) level E_{total} = −52.298875 au. [b] At the CCSD(T)/6-311+G(2df) level E_{total} = −52.296998 au. [c] Infrared intensities in km/mol are shown in parentheses.

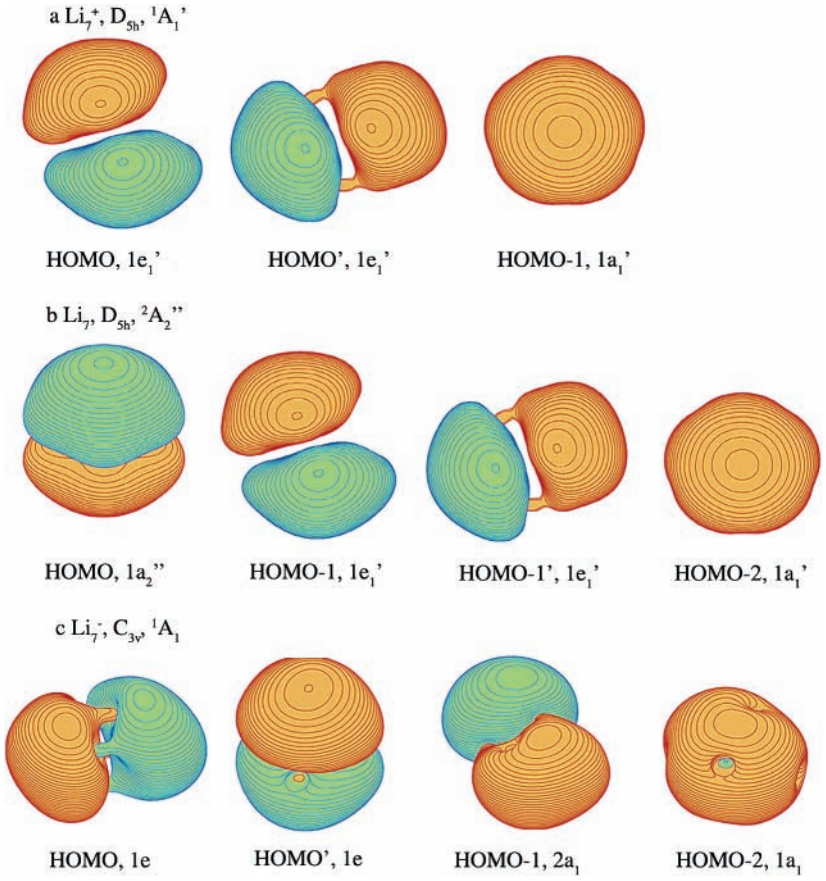

Figure 7. Molecular orbital picture of low-lying heptaatomic lithium clusters.

($1e_u$), and it also has one electron on the π-HOMO ($1a_{2u}$) and thus this anion could be considered as partially π-aromatic.

In the case of charged and neutral Li_6 clusters, the computed NICS indices agree with our interpretation of the chemical bonding. The aromaticity of Li_6 and Li_6^- (negative NICS) and antiaromaticity of Li_6^+ (positive NICS) are identified.

$Li_7^{+1/0/-1}$. MOs of heptaatomic clusters are shown in Figure 7. The molecular orbitals of the Li_7^+ global minimum species are shown in Figure 7a. They have a distinct σ-character. $1a_1'$ HOMO-1 is a completely bonding MO, while the doubly degenerate $1e_1'$ HOMO has one nodal plane and possesses partially bonding character. This provides a sufficient number of electrons for the five-member ring of the system to be σ-aromatic and, consequently, to possess extra stability.

The global minimum isomer of the neutral Li_7 cluster, having D_{5h}, $^2A_2''$ symmetry, is very similar to the cationic

Table 10. Calculated Nucleus-Independent Chemical Shift (NICS) Values for the Global Minima of the $Li_n^{0/+1/-1}$ ($n = 5-7$) Clusters (B3LYP/6-311+G* Level)

	NICS, ppm									
	Li_5^+ D_{3h}, $^1A_1'$	Li_5 C_{2v}, $^2B_1$	Li_5^- D_{3h}, $^3A_1'$	Li_5^- C_{4v}, $^1A_1$	Li_6^+ C_{2v}, $^2A_1$	Li_6 D_{4h}, $^1A_{1g}$	Li_6^- D_{4h}, $^1A_{2u}$	Li_7^+ D_{5h}, $^1A_1'$	Li_7 D_{5h}, $^2A_2''$	Li_7^- D_{5h}, $^1A_1'$
1	15.495[a]	−378.466[b]	37.042[a]	4.846[c]	2.868[d]	−1.522[a]	−10.426[a]	−6.598[a]	−10.336[a]	−27.621[a]
2	14.596	−375.088	37.164	4.820	2.158	−1.450	−10.425	−6.544	−10.506	−27.162
3	12.071	−375.614	37.311	4.663	1.370	−1.165	−10.391	−6.546	−10.726	−25.704
4	8.517	−376.467	37.353	4.395	0.598	−0.765	−10.267	−6.669	−10.671	−23.126
5	4.015	−372.000	36.947	4.013	0.074	−0.656	−10.002	−6.515	−10.079	−19.591
6	0.561	−359.617	35.908	3.486	3.534	−1.048	−9.549	−5.849	−8.968	−15.688
7		−378.466			3.650					
8		−384.207			3.112					
9		−394.547			2.016					
10		−406.860			1.122					
11		−417.223			2.373					
12		−417.144			0.756					
13					−1.396					
14					−3.364					
15					−4.593					

[a] The first index is computed at the center of the symmetry of the polyhedron. The subsequent indices are computed at the points lying equidistantly on the line connecting point 1 and the center of the circle circumscribed around the face of the polyhedron so that points 2−4 are inside of the cluster, point 5 is at the center of the circumscribed circle, and point 6 is outside of the cluster. [b] The first index is computed at the center of the polyhedron. Indices 2−6 and 7−12 are computed at the points lying equidistantly on the lines connecting point 1 and the center of the circle circumscribed around the face Li1−Li2−Li3 and around the face Li1−Li3−Li4, respectively. Points 2−4 and 7−10 are inside of the cluster, points 5 and 11 are at the centers of the circumscribed circles, and points 6 and 12 are outside of the cluster. [c] The first index is computed at the center of the base of the pyramid. The subsequent indices are computed at the points lying equidistantly on the line connecting point 1 and the center of the circle circumscribed around the face of the pyramid so that points 2−4 are inside of the cluster, point 5 is at the center of the circumscribed circle, and point 6 is outside of the cluster. [d] The first index is computed at the point between atoms Li3 and Li4, structure IX, Figure 3. Indices 1−5 are computed at the points lying on the line orienting downward from point 1. Indices 6−10 and 11−15 are computed at the points lying equidistantly on the lines connecting point 1 and the center of the circle circumscribed around the face Li3−Li2−Li5 and around the face Li3−Li5−Li6, respectively. Points 6−8 and 11−13 are inside of the cluster, points 9 and 14 are at the centers of the circumscribed circles, and points 10 and 15 are outside of the cluster.

species XV described above. Out of the four occupied molecular orbitals depicted in the Figure 7b, HOMO-1 ($1e_1'$) and HOMO-2 ($1a_1'$) have the same shapes as the HOMO and HOMO-1, respectively, in the Li_7^+ global minimum moiety. For the reason explained above the species is σ-aromatic. The singly occupied HOMO ($1a_2''$) also contributes to the overall stabilization of the system. This is a completely bonding molecular orbital of π-character. The system, even though having only one π-electron, can be called partially π-aromatic. Thus, the species is doubly aromatic.

The electronic configuration of the global minimum of the Li_7^- (D_{5h}, $^1A_1'$) cluster differs from the Li_7 (D_{5h}, $^2A_2''$) system only by the double population of the HOMO ($1a_2''$). The molecular orbital picture is identical to the one in Figure 7b. Using the same arguments, we conclude that the global minimum of the Li_7^- has doubly aromatic character of the chemical bonding due to the presence of six σ-electrons and two π-electrons. The four valence molecular orbitals in the Li_7^- D_{5h} cluster can also be considered as affective s (HOMO-2, $1a_1'$), p_x (HOMO-1, $1e_1'$), p_y (HOMO-1′, $1e_1'$), and p_z (HOMO, $1a_2''$) orbitals of the superatom, and complete occupation of these orbitals corresponds to major electron-shell closure (compare for example to Ne). And this result is also similar to the jellium model prediction for $n = 8$.[94]

From Figure 7c, where the populated molecular orbitals of the C_{3v}, $^1A_1$ Li_7^- species are shown, one may see that there is no electron density observed on the lithium atom coordinated at the face of the pyramid. The completely bonding HOMO-2 ($1a_1$) contains two σ-electrons and makes the system σ-aromatic according to the ($4n+2$) Hückel's rule. The remaining three molecular orbitals have an obvious triply degenerate nature of the octahedrally symmetric unit, which lost its symmetry due to the presence of the coordinated Li atom changing the point group of the cluster to the C_{3v}. The 1e HOMO and the $2a_1$ HOMO-1 are mostly composed of the 2p-atomic orbitals of the four Li atoms with 2s-contribution from the other two apex Li atoms and have primarily π-character. The complete occupation of this quasi-triply degenerate set leads to the symmetry, stability, and three-dimensional aromaticity of the cluster.

On the basis of negative NICS indices (see Table 10), the assigned aromaticity of all pentagonal bipyramids Li_7^+, Li_7, and Li_7^- receives additional confirmation. Moreover, according to NICS values, the aromatic character of the clusters grows upon addition of electrons to the aromatic π-MO (HOMO in Li_7 and Li_7^-), which is also in accordance with our conclusion about the gain of π-aromaticity.

V. Conclusions

We demonstrated on the small lithium clusters $Li_n^{0/+1/-1}$ ($n = 5-7$) that the novel Gradient Embedded Genetic Algorithm (GEGA) technique can be successfully used for identifying the lowest-energy structures. Results of our search, obtained using this program, have been compared with the previous ab initio calculations and experiments, and

the efficiency of the developed GEGA method has thus been confirmed. We plan to use the GEGA method for search for global minimum and low-lying structures of many main group elements' clusters. From the MO analysis of the chemical bonding in the clusters, found via the novel GEGA program, the significant role of multiple aromaticity as a major stabilizing effect in alkali-metal clusters has been elucidated. Our interpretation of aromatic or antiaromatic character of lithium clusters does not always agree with the assignments based on the computed NICS indices. In our previous work we reported the smaller systems of alkali and alkaline Earth metals and showed the importance of the σ-aromaticity concept in the description of the chemical bonding within them.[72] In this work we extend our knowledge about clusters of alkali metals, increasing the size of the considered systems.

Acknowledgment. This work was supported partially by the donors of the Petroleum Research Fund (ACS-PRF# 38242-AC6), administered by the American Chemical Society and partially by the National Science Foundation (CHE-0404937). The authors express their gratitude to Loren Hasen for discussions on the genetic algorithm technique.

References

(1) Holland, J. H. *Adaptation in Natural and Artificial Systems;* The University of Michigan Press: Ann Arbor, 1975.

(2) Goldberg, D. E. *Genetic Algorithms in Search, Optimization, and Machine Learning*; Addison-Wesley: Reading, MA, 1989.

(3) Davis, L. *Handbook of Genetic Algorithms*; Van Nostrand Reinhold: New York, 1991.

(4) Wang, J. L.; Wang, G. H.; Zhao, J. J. *Rhys. Rev. B* **2002**, *66*, 035418.

(5) Wang, J. L.; Wang, G. H.; Zhao, J. J. *Phys. Rev. A* **2003**, *68*, 013201.

(6) Gregurick, S. K.; Alexander, M. H.; Hartke, B. *J. Chem. Phys.* **1996**, *104(7)*, 2684.

(7) White, R. P.; Niesse, J. A.; Mayne, H. R. *J. Chem. Phys.* **1998**, *108(5)*, 2208.

(8) Marim, L. M.; Lemes, M. R.; Dal Pino, A., Jr. *Phys. Rev. A* **2003**, *67*, 033203.

(9) Ho, K. M.; Shvartsburg, A. A.; Pan, B.; Lu, Z. Y.; Wang, C. Z.; Wacker, J. G.; Fye, J. L.; Jarrold, M. F. *Nature* **1998**, *392*, 582.

(10) Cai, W.; Jiang, H.; Shao, X. *J. Chem. Inf. Comput. Sci.* **2002**, *42*, 1099.

(11) Stucke, D. P.; Crespi, V. H. *Nano Lett.* **2003**, *3*, 9, 1183.

(12) Haupt, R. L.; Haupt, S. E. *Practical Genetic Algorithms;* Wiley-Interscience Publication, John Wiley & Sons: New York, Chichester, Weinheim, Brisbane, Singapore, Toronto, 1998.

(13) Deaven, D. M.; Ho, K. M. *Phys. Rev. Lett.* **1995**, *75*, 2, 288.

(14) Zairi, Y. *Phys. Rev. E* **1995**, *51*, 4, R2769.

(15) Morris, J. R.; Deaven, D. M.; Ho, K. M. *Phys Rev. B* **1996**, *53*, R1740.

(16) Tomasulo, A.; Ramakrishna, M. V. *J. Chem. Phys.* **1996**, *105*, 23, 10449.

(17) Niesse, J. A.; Mayne, H. R. *J. Chem. Phys.* **1996**, *105*, 11, 4700.

(18) Wang, G. M.; Blaisten-Barojas, E.; Roitberg, A. E. *J. Chem. Phys.* **2001**, *115*, 8, 3640.

(19) Iwamatsu, M. *J. Chem. Phys.* **2000**, *112*, 24, 10976.

(20) Yoo, S.; Zeng, X. C. *J. Chem. Phys.* **2003**, *119*, 3, 1442.

(21) Guimaraes, F. F.; Belchior, J. C.; Johnston, R. L.; Roberts, C. *J. Chem. Phys.* **2002**, *116*, 19, 8327.

(22) Hui, L.; Pederiva, F.; Wang, G. H.; Wang, B. L. *J. Chem. Phys.* **2003**, *119*, 18, 9771.

(23) Lai, S. K.; Hsu, P. J.; Wu, K. L.; Liu, W. K.; Iwamatsu, M. *J. Chem. Phys.* **2002**, *117*, 23, 10715.

(24) Bazterra, V. E.; Ferraro, M. B.; Facelli, J. C. *J. Chem. Phys.* **2002**, *116*, 14, 5984.

(25) Bobadovaa-Parvanova, P.; Jackson, K. A.; Srinivas, S.; Horoi, M.; Kohler, C.; Seifert, G. *J. Chem. Phys.* **2002**, *116*, 9, 3576.

(26) Darby, S.; Mortimer-Jones, T. V.; Johnston, R. L.; Roberts, C. *J. Chem. Phys.* **2002**, *116*, 4, 1536.

(27) Kabrede, H.; Hentschke, R. *J. Phys. Chem. B* **2003**, *107*, 3914−3920.

(28) Kabrede, H.; Hentschke, R. *J. Phys. Chem. B* **2002**, *106*, 10089−10095.

(29) Dugourd, P.; Rayane, D.; Labastie, P.; Vezin, B.; Chevaleyre, J.; Broyer, M. *Chem. Phys. Lett.* **1992**, *97*, 433.

(30) Benichou, E.; Allouche, A. R.; Aubert-Frecon, M.; Antoine, R.; Broyer, M.; Dugourd, Ph.; Rayane, D. *Chem. Phys. Lett.* **1998**, *290*, 171.

(31) Bonacic-Koukecky, V.; Pittner, J.; Fuchs, C.; Fantucci, P.; Koutecky, J. *NATO Sci. Ser., Ser. C* **1992**, *372* (Phys. Chem. Finite Syst,: Clusters Cryst., Vol. 2), 899.

(32) Fantucci, P.; Bonacic-Koukecky, V.; Jellinek, J.; Wiechert, M.; Harrison, R. J.; Guest, M. F. *Chem. Phys. Lett.* **1996**, *250*, 47.

(33) Howard, J. A.; Joly, H. A.; Jones, R.; Edwards, P. P.; Singer, R. J.; Logan, D. E. *Chem. Phys. Lett.* **1993**, *204*, 128.

(34) Szaniszlo, J.; Tamassy-Lentei, I. *Acta Phys. Chim. Debrecina* **1994**, *29*, 25.

(35) Rousseau, R.; Marx, D. *Phys. Rev. A* **1997**, *56*, 617.

(36) Gibson, D. A.; Carter, E. A. *Chem. Phys. Lett.* **1997**, *271*, 266.

(37) Chihaia, V.; Sandu, T.; Vass, M. *Rom. J. Phys.* **1998**, *43*, 409.

(38) Fournier, R.; Chang, J. B. Y.; Wong, A. *J. Chem. Phys.* **2003**, *119*, 9444.

(39) de Visser, S. P.; Alpert, Y.; Danovich, D.; Shaik, S. *J. Phys. Chem. A* **2000**, *104*, 11223.

(40) Rousseau, R.; Marx, D. *J. Chem. Phys.* **1999**, *111*, 5091.

(41) Jones, R. O.; Lichtenstein, A. I.; Hutter, J. *J. Chem. Phys.* **1997**, *106*, 4566.

(42) Gardet, G.; Rogemond, F.; Chetmett, H. *Theor. Chim. Acta* **1995**, *91*, 249.

(43) Gardet, G.; Rogemond, F.; Chetmett, H. *J. Chem. Phys.* **1996**, *105*, 9933.

(44) Quassowski, S.; Hermann, K. *Phys. Rev. B* **1995**, *51*, 2457.

(45) Kawai, R.; Tombrello, J. F.; Weare, J. H. *Phys. Rev. A* **1994**, *49*, 4236.

(46) Lin, Z.; Slee, T.; Mingos, D. M. P. *Chem. Phys.* **1990**, *142*, 321.

(47) Ishi, S.; Ohno, K.; Kawazoe, Y.; Louie, S. G. *Phys. Rev. B* **2002**, *65*, 245109.

(48) Blank, J.; Bonacic-Koukecky, V.; Broyer, M.; Chevaleyre, J.; Dugourd, P.; Koutechy, J.; Scheuch, C.; Wolf, J. P.; Woeste, L. *J. Chem. Phys.* **1992**, *96*, 1793.

(49) Boustani, I.; Pewestorf, W.; Fantucci, P.; Bonacic-Koukecky, V.; Koutechy, J. *Phys. Rev. B* **1987**, *35*, 9437.

(50) Bauschlicher, C. W., Jr. *Chem. Phys.* **1996**, *206*, 35.

(51) Maynau, D.; Malrieu, J. P. *J. Chem. Phys.* **1988**, *88*, 3163.

(52) Grassi, A.; Loombardo, G. M.; Angilella, G. G. N.; March, N. H.; Pucci, R. *J. Chem. Phys.* **2003**, *120*, 24, 11615.

(53) de Visser, S. P.; Danovich, D.; Wu, W.; Shaik, S. *J. Phys. Chem. A* **2002**, *106*, 4961.

(54) de Visser, S. P.; Alpert, Y.; Danovich, D.; Shaik, S. *J. Phys. Chem. A* **2000**, *104*, 11223.

(55) Danovich, D.; Wu, W.; Shaik, S. *J. Am. Chem. Soc.* **1999**, *121*, 3165.

(56) Temelso, B.; Sherrill, C. D. *J. Chem. Phys.* **2005**, *122*, 064315.

(57) Li, X. W.; Pennington, W. T.; Robinson, G. H. *J. Am. Chem. Soc.* **1995**, *117*, 7578.

(58) Li, X. W.; Xie, Y.; Schreiner, P. R.; Gripper, K. D.; Crittendon, R. C.; Campana, C. F.; Schaefer, H. F.; Robinson, G. H. *Organometallics* **1996**, *15*, 3798.

(59) Xie, Y.; Schreiner, P. R.; Schaefer, H. F. III; Li, X. W.; Robinson, G. H. *J. Am. Chem. Soc.* **1995**, *117*, 7578.

(60) Li, X.-W.; Xie, Y.; Schreiner, P. R.; Gripper, K. D.; Crittendon, R. C.; Campana, C. F.; Schaefer, H. F.; Li, X. W.; Robinson, G. H. *Organometallics* **1996**, *15*, 3798.

(61) Robinson, G. H. *Acc. Chem. Res.* **1999**, *32*, 773.

(62) Li, X.; Kuznetsov, A. E.; Zhang, H. F.; Boldyrev, A. I.; Wang L. S. *Science* **2001**, *291*, 859.

(63) Li, X.; Zhang, H. F.; Wang, L. S.; Kuznetsov, A. E.; Cannon, N. A.; Boldyrev, A. I. *Angew. Chem., Int. Ed.* **2001**, *40*, 1867.

(64) Kuznetsov, A. E.; Corbett, J. D.; Wang, L. S.; Boldyrev, A. I. *Angew. Chem., Int. Ed.* **2001**, *40*, 3369.

(65) Kuznetsov, A. E.; Boldyrev, A. I.; Li, X.; Wang, L. S. *J. Am. Chem. Soc.* **2001**, *123*, 8825.

(66) Boldyrev, A. I.; Kuznetsov, A. E. *Inorg. Chem.* **2002**, *41*, 532.

(67) Kuznetsov, A. E.; Boldyrev, A. I.; Zhai, H.-J.; Wang, L. S. *J. Am. Chem. Soc.* **2002**, *124*, 11791.

(68) Zhan, C.-G.; Zhan, F.; Dixon, D. A. *J. Am. Chem. Soc.* **2002**, *124*, 14795.

(69) Fowler, P. W.; Havenith, R. W. A.; Steiner, E. *Chem. Phys. Lett.* **2001**, *342*, 85.

(70) Fowler, P. W.; Havenith, R. W. A.; Steiner, E. *Chem. Phys. Lett.* **2001**, *359*, 530.

(71) Juselius, J.; Straka, M.; Sundholm, D. *J. Phys. Chem. A* **2001**, *105*, 9939.

(72) Alexandrova, A. N.; Boldyrev, A. I. *J. Phys. Chem. A* **2003**, *107*, 554−560.

(73) Gaussian 03, Revision C.02, Frisch, M. J.; Trucks, G. W.; Schlegel, H. B.; Scuseria, G. E.; Robb, M. A.; Cheeseman, J. R.; Montgomery, J. A., Jr.; Vreven, T.; Kudin, K. N.; Burant, J. C.; Millam, J. M.; Iyengar, S. S.; Tomasi, J.; Barone, V.; Mennucci, B.; Cossi, M.; Scalmani, G.; Rega, N.; Petersson, G. A.; Nakatsuji, H.; Hada, M.; Ehara, M.; Toyota, K.; Fukuda, R.; Hasegawa, J.; Ishida, M.; Nakajima, T.; Honda, Y.; Kitao, O.; Nakai, H.; Klene, M.; Li, X.; Knox, J. E.; Hratchian, H. P.; Cross, J. B.; Bakken, V.; Adamo, C.; Jaramillo, J.; Gomperts, R.; Stratmann, R. E.; Yazyev, O.; Austin, A. J.; Cammi, R.; Pomelli, C.; Ochterski, J. W.; Ayala, P. Y.; Morokuma, K.; Voth, G. A.; Salvador, P.; Dannenberg, J. J.; Zakrzewski, V. G.; Dapprich, S.; Daniels, A. D.; Strain, M. C.; Farkas, O.; Malick, D. K.; Rabuck, A. D.; Raghavachari, K.; Foresman, J. B.; Ortiz, J. V.; Cui, Q.; Baboul, A. G.; Clifford, S.; Cioslowski, J.; Stefanov, B. B.; Liu, G.; Liashenko, A.; Piskorz, P.; Komaromi, I.; Martin, R. L.; Fox, D. J.; Keith, T.; Al-Laham, M. A.; Peng, C. Y.; Nanayakkara, A.; Challacombe, M.; Gill, P. M. W.; Johnson, B.; Chen, W.; Wong, M. W.; Gonzalez, C.; Pople, J. A. Gaussian, Inc., Wallingford CT, 2004.

(74) Parr, R. G.; Yang, W. *Density-functional theory of atoms and molecules*; Oxford University Press: Oxford, 1989.

(75) Becke, A. D. *J. Chem. Phys.* **1993**, *98*, 5648.

(76) Perdew, J. P.; Chevary, J. A.; Vosko, S. H.; Jackson, K. A.; Pederson, M. R.; Singh, D. J.; Fiolhais, C. *Phys. Rev. B* **1992**, *46*, 6671.

(77) Hammersley, J. M.; Handscomb, D. C. *Monte Carlo Methods*; Methuen: London, 1965; Chapter 9.

(78) Cizek, J. *Adv. Chem. Phys.* **1969**, *14*, 35.

(79) Purvis, G. D, III; Bartlett, R. J. *J. Chem. Phys.* **1982**, *76*, 1910.

(80) Scuseria, G. E.; Janssen, C. L.; Schaefer, H. F., III *J. Chem. Phys.* **1988**, *9*, 7282.

(81) Raghavachari, K.; TrucksJohn, G. W. A.; Pople, J. A.; Head-Gordon, M. *Chem. Phys. Lett.* **1989**, *157*, 479.

(82) Bartlett, R. J.; Watts, J. D.; Kucharski, S. A.; Noga, J. *Chem. Phys. Lett.* **1990**, *165*, 513.

(83) Schaftenaar, G. MOLDEN3.4, CAOS/CAMM Center, The Netherlands 1998.

(84) NPA Version 3.1, Reed, A. E., Carpenter, J. E.; Weinhold, F.; 1998.

(85) Schleyer, P. v. R.; Maerker, C.; Dransfeld, A.; Jiao, H.; van Eikema Hommes, N. J. R. *J. Am. Chem. Soc.* **1996**, *118*, 6317.

(86) Huber, K. P.; Herzberg, G. *Molecular Spectra and Molecular Structure. IV. Constants of Diatomic Molecules*; Van Nostrand: New York, 1979.

(87) While π-aromaticity and π-antiaromaticity, when delocalized bonding occurs due to the π-overlap of atomic orbitals, are well-known, σ-(anti)aromaticity is less known in chemistry. σ-aromaticity occurs when the number of σ-electrons is not sufficient for population of σ-MOs, which could be localized in classical 2c-2e bonds. It has been introduced by Dewar.[88] Double aromaticity (the simultaneous presence of σ- and π-aromaticity) was introduced in chemistry by Schleyer and co-workers[89] in the late 1970s for explaining properties of the 3,5-dehydrophenyl cation. Double aromaticity and anti-aromaticity was first used by Martin-Santamaria and Rzepa[90]

for explaining chemical bonding in small carbon rings. Berndt and co-workers have shown that small carborane molecules containing three- and four-membered rings also exhibit both σ and π aromaticity.[91]

(88) (a) Dewar, M. J. S. *Bull. Soc. Chim. Belg.* **1979**, *88*, 957. (b) Dewar, M. J. S.; McKee, M. L. *Pure Appl.* Chem. **1980**, *52*, 1431. (c) Dewar, M. J. S. *J. Am. Chem. Soc.* **1984**, *106*, 669.

(89) Chandrasekhar, J.; Jemmis, E. D.; Schleyer, P. v. R. *Tetrahedron Lett.* **1979**, *39*, 3707.

(90) Martin-Santamaria, S.; Rzepa, H. S. *Chem. Commun.* **2000**, *16*, 1503.

(91) (a) Präsang, C.; Mlodzianowska, A.; Sahin, Y.; Hofmann. M.; Geiseler. G.; Massa, W.; Berndt. A. *Angew. Chem. Int. Ed.* **2002**, *41*, 3380. (b) Präsang, C.; Hofmann. M.; Geiseler. G.; Massa, W.; Berndt, A. *Angew. Chem. Int. Ed.* **2002**, *41*, 1526. (c) Präsang, C.; Mlodzianowska, A.; Geiseler, G.; Massa, W.; Hofmann, M.; Berndt, A. *Pure Appl. Chem.* **2003**, 75, 1175. (d) Amseis, P.; Mesbah, W.; Präsang, C.; Hofmann, M.; Geiseler, G.; Massa, W.; Berndt, A. *Organometallics* **2003**, *22*, 1594. (e) Mesbah, W.; Präsang, C.; Hofmann, M.; Geiseler, G.; Massa, W.; Berndt, A. *Angew. Chem., Int. Ed.* **2003**, *42*, 1717.

(92) Li, X.; Kuznetsov, A. E.; Zhang, H. F.; Boldyrev, A. I.; Wang, L. S. *Science* **2001**, *291*, 859.

(93) Gogonea, V.; Schleyey, P. v. R.; Scheiner, P. R. *Angew. Chem., Int. Ed.* **1998**, *37*, 1945.

(94) Knigh, W. D.; Clemenger, K.; de Heer, W. A.; Saunders: W. A.; Cho, M. Y.; Cohen, M. L. *Phys. Rev. Lett.* **1984**, *52*, 2141.

CT050093G